NANOSYSTEMS:
PHYSICS, CHEMISTRY, MATHEMATICS

Kozlov S.S., et al. *Nanosystems: Phys. Chem. Math.*, 2023, **14** (5), 584–589.
http://nanojournal.ifmo.ru
DOI 10.17586/2220-8054-2023-14-5-584-589

Original article

Planar perovskite solar cells with La_2NiMnO_6 buffer layer

Sergey S. Kozlov[1], Anna B. Nikolskaia[1], Olga K. Karyagina[1], Ekaterina K. Kosareva[2], Olga V. Alexeeva[1], Vasilisa I. Petrova[1], Oksana V. Almjasheva[3,4], Oleg I. Shevaleevskiy[1]

[1]Emanuel Institute of Biochemical Physics, Russian Academy of Sciences, Moscow, Russia

[2]N. N. Semenov Federal Research Center for Chemical Physics, Russian Academy of Science, Moscow, Russia

[3]St. Petersburg State Electrotechnical University "LETI", St. Petersburg, Russia

[4]Ioffe Physical-Technical Institute, Russian Academy of Sciences, St. Petersburg, Russia

Corresponding author: Anna B. Nikolskaia, anickolskaya@mail.ru

PACS 84.60.Jt

ABSTRACT Thin films of La_2NiMnO_6 (LNMO) double perovskite oxide were first used as buffer layers in planar perovskite solar cells (PSCs) with the architecture of glass/FTO/LNMO/$CH_3NH_3PbI_3$/Spiro-MeOTAD/Au. All PSCs were fabricated under ambient conditions and their photovoltaic parameters were measured under standard illumination (AM1.5G, 1000 W/m^2). Power conversion efficiency (PCE) values (10 – 11 %) for the PSCs developed were comparable with those obtained for conventional PSCs with compact TiO_2 ($cTiO_2$) layer, but the stability of PSCs with LNMO buffer layer was significantly higher than for $cTiO_2$-based PSCs.

KEYWORDS nanostructures, double perovskite oxides, perovskite solar cells, solar photovoltaics

ACKNOWLEDGEMENTS This work was supported by the Russian Science Foundation under grant No. 20-69-47124.

FOR CITATION Kozlov S.S., Nikolskaia A.B., Karyagina O.K., Kosareva E.K., Alexeeva O.V., Petrova V.I., Almjasheva O.V., Shevaleevskiy O.I. Planar perovskite solar cells with La_2NiMnO_6 buffer layer. *Nanosystems: Phys. Chem. Math.*, 2023, **14** (5), 584–589.

1. Introduction

The search and development of new types of solar cells with high efficiency and stability is one of the most urgent tasks of the modern photovoltaics [1,2]. In the last decade, the great interest has been focused on the studies of perovskite solar cells (PSCs), in which hybrid organic-inorganic materials, such as $CH_3NH_3PbX_3$ (X = Cl^-, Br^- or I^-), are used as photosensitive layers. Improvement of the PSC fabrication technology allowed one to achieve high values of power conversion efficiency (PCE), which nowadays exceeds 25 % [3–5]. Low cost and simple manufacturing methods make PSCs a promising alternative to traditional silicon-based solar cells. However, perovskite materials used in PSCs are characterized by low stability and degrade under ambient conditions or under continuous illumination. As a result, PCE of PSCs is significantly decreased over time, which limits the application prospects [6, 7].

Previously, it was shown that the highest PCE values can be achieved using PSCs with a planar structure [8, 9]. The architecture of the state-of-the-art planar PSC sample is glass/FTO/$cTiO_2$/$CH_3NH_3PbI_3$/SpiroMeOTAD/Au, where FTO is a fluorine-doped tin oxide conductive coating (F:SnO_2), $cTiO_2$ is a compact layer of TiO_2 nanoparticles with the thickness $\sim$ 50 nm. The functions of $cTiO_2$ layer include blocking hole transfer from the perovskite material to the FTO coating and preventing direct contact between $CH_3NH_3PbI_3$ layer and the FTO surface [10, 11]. However, PSCs with planar structure were found to be the most sensitive to external factors such as humidity, temperature, and illumination. The latter is due to both the degradation of the perovskite material itself and the instability of the TiO_2 layer when exposed to ultraviolet radiation. Long-term illumination causes desorption of oxygen molecules inside the TiO_2 material, which initiate the degradation of the perovskite layer [12–14]. In addition, FTO layer is characterized by relatively rough and non-uniform surface, which may lead to non-uniform deposition of $cTiO_2$ layer on FTO substrate. The latter causes the appearance of morphological defects in the perovskite layer deposited on top of FTO/$cTiO_2$ substrate, which also initiates rapid degradation of PSCs [12, 13]. In the literature, attempts to reduce the degradation effects in PSCs by applying $CH_3NH_3PbI_3$ layer directly to the FTO coating were described, but this leaded to the decrease in PCE values [15, 16]. Thus, nowadays an important task for PSC improvement is to find new materials suitable for use in planar PSC as a buffer layer that do not contribute to the degradation of perovskite material.

In this work, a highly stable inorganic material such as double perovskite oxide La_2NiMnO_6 (LNMO) was first used as a buffer layer in planar PSCs. The LNMO thin films on glass substrates were obtained by spin coating and were

investigated using optical spectroscopy and X-ray diffraction techniques, as well as atomic force microscopy (AFM). Planar PSCs with the architecture of glass/FTO/LNMO/$CH_3NH_3PbI_3$/Spiro-MeOTAD/Au were fabricated under ambient conditions at high humidity level ($\sim$ 50 %) and their photovoltaic (PV) parameters were measured. The data obtained demonstrate a new approach to PSCs optimization for long-term operation in outdoor conditions.

2. Experimental

2.1. Buffer layer preparation

The appropriate amounts of $La(NO_3)_3 \cdot 6H_2O$, $Ni(NO_3)_2 \cdot 6H_2O$ and $Mn(NO_3)_2 \cdot 6H_2O$ powders were dissolved in a mixture of 2-ethoxyethanol and acetic acid (4:1 v/v) to obtain 0.3 M stock solution. The LNMO thin films were obtained by spin coating of the stock solution on the surface of non-conductive glass substrates (3000 rpm, 30 s), followed by annealing at 550 – 650 °C during 2 hrs in the muffle furnace. The obtained LNMO thin films were used for XRD, AFM and optical measurements. LNMO-based buffer layers were deposited on the FTO-glass substrates following the same spin coating and annealing protocols using the 5-fold diluted stock solution and were used further for PSCs fabrication. FTO glass substrates coated by $cTiO_2$ layer were obtained following the technique described in [17].

2.2. Device fabrication

Planar PSCs were fabricated under ambient conditions at relatively high humidity level ($\sim$ 50 – 60 %) according to the procedure described in [18]. Perovskite ($CH_3NH_3PbI_3$) layer was formed on the surface of LNMO layer using a conventional one-step deposition method [19]. A layer of Spiro-MeOTAD hole transport material was spin-coated onto the surface of the perovskite layer (3000 rpm, 20 s). The final stage of PSC fabrication was the deposition of $\sim$ 50-nm thick Au contacts by vacuum thermal evaporation using the VUP-4 vacuum post. Schematic representation of the PSC architecture is illustrated in Fig. 1. The state-of-the-art planar PSCs were fabricated using FTO glass substrates coated by $cTiO_2$ layer via the same technique as described above [18].

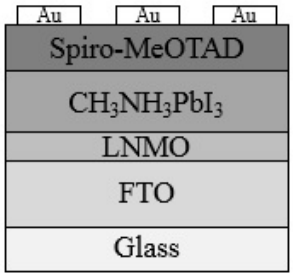

FIG. 1. Schematic representation of the planar PSC architecture

3. Characterization studies

The X-ray diffraction (XRD) measurements of LMNO thin films were provided using DRON-3M X-ray diffractometer with Cu Kα radiation ($\lambda = 1.5405$ Å) as the X-ray source. Atomic force microscope (AFM) NTEGRA Prima (NT-MDT) with HA_NC probes (TipsNano, resonant frequency 140 kHz, stiffness constant 3.5 N/m) was used to investigate the surface morphology and to evaluate average particle size in LNMO thin films. The optoelectronic properties of the LNMO layers were studied using UV-Vis spectrophotometer (Shimadzu UV-3600, Japan) with an ISR-3100 integrating sphere in the wavelength range of 300 – 1400 nm.

Photovoltaic (PV) characteristics of the developed PSCs were measured under standard illumination conditions (AM1.5G, 1000 W/m^2) by recording the current density-voltage (J–V) characteristics using Keithley 4200-SCS Semiconductor Characterization System (Keithley, USA) and Abet Technologies 10500 solar simulator with Xenon lamp (Abet, USA) as the light source. The PCE (η) values of the PSCs were calculated from the J–V data using the known formula [20]:

$$\eta = \frac{J_{SC} \cdot V_{OC} \cdot FF}{P_{IN}} \cdot 100\ \%, \tag{1}$$

where J_{SC} – short-circuit current density, V_{OC} – open-circuit voltage, FF – fill factor and P_{IN} – incoming light intensity.

4. Results and discussion

XRD patterns of the LNMO thin films deposited on non-conductive glass substrates and annealed at different temperatures (550 – 650 °C) are shown in Fig. 2(a). LNMO films obtained at 575 – 650 °C showed XRD reflexes corresponding to monoclinic, rhombohedral and orthorhombic phases of LNMO, confirming the triple phase structure of La_2NiMnO_6 double perovskite oxides [21]. The absence of additional XRD peaks indicates the purity of the samples. In contrast, LNMO film obtained at 550 °C was found to possess amorphous structure.

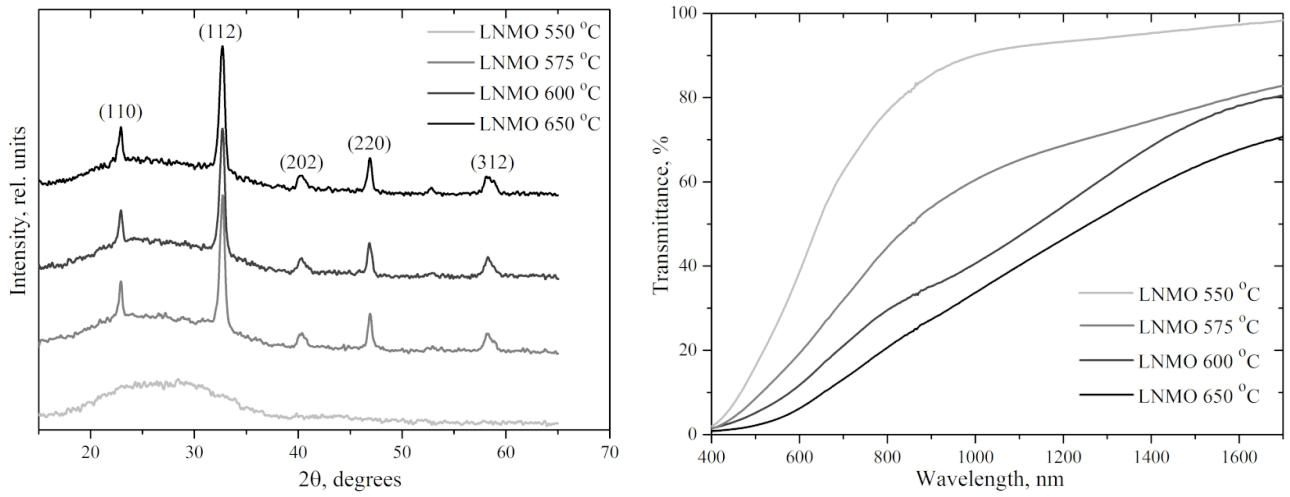

FIG. 2. XRD patterns (a) and transmittance spectra (b) of LNMO thin films, obtained at different annealing temperatures

Transmittance spectra for LNMO thin films deposited on the surface of non-conductive glass substrates is shown on Fig. 2(b). Using these data and Tauc equation for direct transitions, the energy bandgap (E_g) values were obtained (Table 1) [22]. It can be seen that an increase in annealing temperature leads to a decrease in the E_g value for the studied LNMO layers from 1.75 to 1.04 eV. As a result, all LNMO samples possesses semiconductor properties.

TABLE 1. The energy bangap (E_g) values calculated for LNMO thin films, obtained at different annealing temperatures (T)

T, °C	550	575	600	650
E_g, eV	1.75	1.50	1.05	1.04

AFM images of LNMO thin layers deposited on FTO glass substrates show that regardless of annealing temperature, fabricated layers are characterized by homogeneous structure with uniform particle distribution (Fig. 3). The average particle size determined using AFM was found to be around 60 – 70 nm. A comparison of the particle size (Fig. 3) and the crystallite size determined from data about the broadening of X-ray diffraction lines indicates that the particles are polycrystalline, consisting of crystallites 15 ± 2 nm in size.

The LNMO thin films fabricated on the surface of FTO conductive glasses were used for fabrication of planar PSCs with the architecture of FTO/LNMO/$CH_3NH_3PbI_3$/Spiro-OMeTAD/Au under ambient conditions. State-of-the-art planar PSC with cTiO_2 layer was constructed for providing comparative analysis. J–V curves recorded under standard illumination (1000 W/m^2, AM1.5G) for PSCs with LNMO and cTiO_2 layers are shown in Fig. 4(a). The PV parameters for all PSCs are listed in Table 2. It can be seen that the PSCs with LNMO layers demonstrated PCE values (10 – 11 %) comparable to the efficiency obtained for conventional TiO_2-based PSCs (Table 2). The highest PCE was observed for the PSC samples with LNMO thin films prepared at annealing temperature 600 °C. The results confirm that LNMO materials can be successfully used as buffer layers in planar PSCs.

PV parameters of planar PSCs with LNMO and cTiO_2 layers were investigated during long-term storage under ambient conditions. The data obtained (Fig. 4(b)) revealed that PSCs with LNMO-based buffer layer demonstrate more stable behavior than PSCs with cTiO_2 layer. Thus when PSCs were exposed under ambient conditions for 35 days, PCE for PSC with LNMO thin film was almost unchanged, while PCE for cTiO_2-PSC decreased more than 60 %.

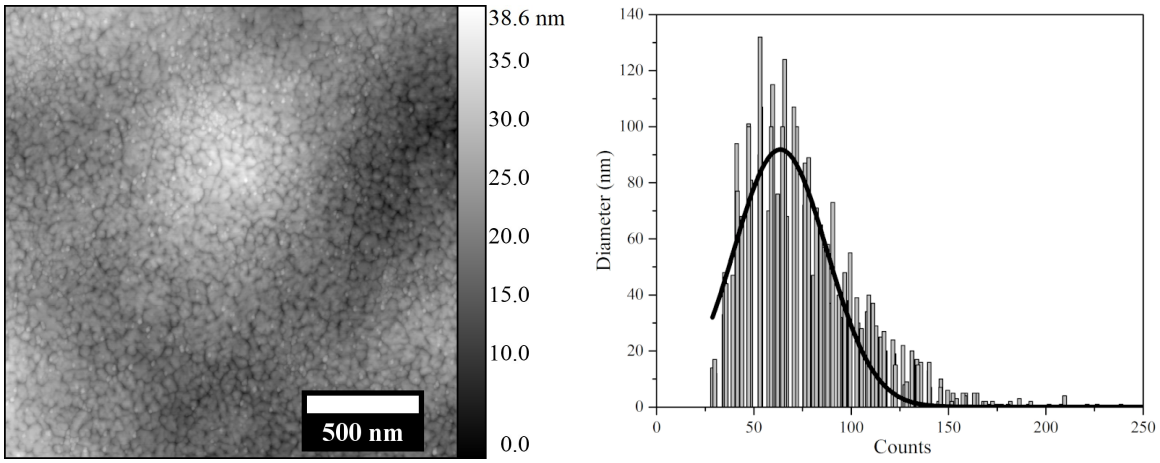

FIG. 3. AFM surface image (left) and particle size distribution (right) for LNMO thin layer obtained at 600 °C

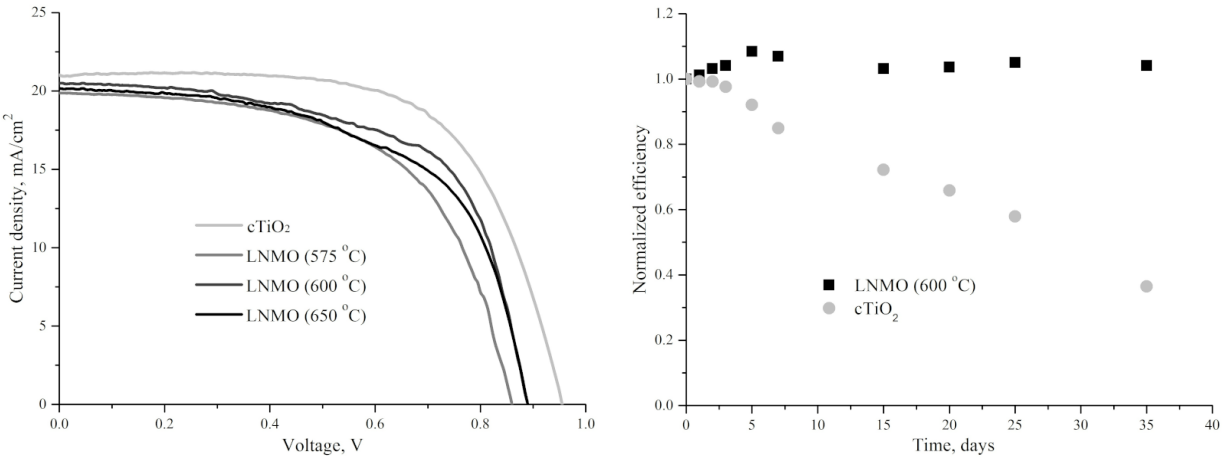

(a) (b)

FIG. 4. J–V curves (a) and stability test (b) for PSCs under standard illumination (1000 W/m^2, AM1.5G)

TABLE 2. The PV parameters for PSCs under standard illumination (1000 W/m^2, AM1.5G)

Sample	J_{SC}, mA/cm^2	V_{OC}, V	FF, a.u.	η, %
PSC with cTiO$_2$	21.0	0.96	0.65	12.6
PSC with LNMO 575 °C	19.3	0.86	0.58	10.0
PSC with LNMO 600 °C	20.5	0.89	0.62	11.4
PSC with LNMO 650 °C	20.2	0.89	0.58	10.5

Summing up, it was shown that La_2NiMnO_6 (LNMO) double perovskite oxide thin films demonstrate semiconductor properties and their optoelectronic characteristics including bandgap values could be easily tuned by changing the synthesis conditions, namely, the annealing temperature. La_2NiMnO_6-based thin films were successfully used as buffer layers in planar PSCs, showing PCE values comparable with those obtained for conventional TiO_2-based PSCs. Due to the high stability of LNMO double perovskite oxides towards moisture and oxygen, incorporation of LNMO buffer layer in PSCs architecture allowed to significantly increase the stability of planar PSCs under ambient conditions as compared to TiO_2-based PSCs behavior.

5. Conclusions

Thin films of La_2NiMnO_6 (LNMO) double perovskite oxide were synthesized on the glass substrates via spin coating and were first used as buffer layers in planar PSCs. LNMO thin films revealed higher homogeneity and stability in comparison with the state-of-the-art $cTiO_2$ layers. The optical and photoelectrical properties of LNMO layers can be tuned by changing the annealing temperature. Planar PSCs with the architecture of FTO/LNMO/$CH_3NH_3PbI_3$/Spiro-OMeTAD/Au were fabricated under ambient conditions. The maximum PCE value of 11.4 % under standard illumination conditions (AM1.5G, 1000 W/m^2) was obtained for PCE with LNMO buffer layer annealed at 600 °C and was comparable to the PCE for PSCs with $cTiO_2$ layer. The stability of PSCs based on LNMO buffer layer was significantly higher than the stability of PSCs with $cTiO_2$ layer. The data obtained demonstrate a novel approach for optimization of PSCs designed for long-term operation in outdoor conditions.

References

[1] Kumar N.S., Naidu K.C.B. A review on perovskite solar cells (PSCs), materials and applications. *J. Materiomics*, 2021, **7**, P. 940–956.
[2] Miah M.H., Rahman M.B., Nur-E-Alam M., Das N., Soin N.B., Hatta S.F.W.M., Islam M.A. Understanding the degradation factors, mechanism and initiatives for highly efficient perovskite solar cells. *Chem. Nano Mat.*, 2023, **9**, e202200471.
[3] Green M.A., Dunlop E.D., Yoshita M., Kopidakis N., Bothe K., Siefer G., Hao X. Solar cell efficiency tables (version 62). *Prog. Photovolt. Res. Appl.*, 2023, **31**, P. 651–663.
[4] Roy P., Kumar Sinha N., Tiwari S., Khare A. A review on perovskite solar cells: evolution of architecture, fabrication techniques, commercialization issues and status. *Sol. Energy*, 2020, **198**, P. 665–688.
[5] Shao J.Y., Li D., Shi J., Ma C., Wang Y., Liu X., Jiang X., Hao M., Zhang L., Liu C., Jiang Y., Wang Z., Zhong Y.W., Liu S.F., Mai Y., Liu Y., Zhao Y., Ning Z., Wang L., Xu B., Meng L., Bian Z., Ge Z., Zhan X., You J., Li Y., Meng Q. Recent progress in perovskite solar cells: material science. *Sci. China Chem.*, 2023, **66**, P. 10–64.
[6] Ahmed S.F., Islam N., Kumar P.S., Hoang A.T., Mofijur M., Inayat A., Shafiullah G.M., Vo D.N., Badruddin I.A., Kamangar S. Perovskite solar cells: thermal and chemical stability improvement, and economic analysis. *Mater. Today Chem.*, 2023, **27**, 101284.
[7] Zhuang J., Wang J., Yan F. Review on chemical stability of lead halide perovskite solar cells. *Nano-Micro Lett.*, 2023, **15**, 84.
[8] Noh M.F.M., Teh C.H., Daik R., Lim E.L., Yap C.C., Ibrahim M.A., Ludin N.A., Yusoff Abd.R.M., Jange J., Teridi M.A.M. The architecture of the electron transport layer for a perovskite solar cell. *J. Mater. Chem. C*, 2018, **6**, P. 682–712.
[9] Wang K., Olthof S., Subhani W. S., Jiang X., Cao Y., Duan L., Wang H., Du M., Liu S. F. Novel inorganic electron transport layers for planar perovskite solar cells: progress and prospective. *Nano Energy*, 2020, **68**, 104289.
[10] Chowdhury T.A., Zafar M.A.B., Islam M.S., Shahinuzzaman M., Islam M.A, Khandaker M.U. Stability of perovskite solar cells: issues and prospects. *RSC Adv.*, 2023, **13**, P. 1787–1810.
[11] Yang G., Tao H., Qin P., Ke W., Fang G. Recent progress in electron transport layers for efficient perovskite solar cells. *J. Mater. Chem. A*, 2016, **4**, P. 3970–3990.
[12] Dipta S.S., Uddin A. Stability Issues of perovskite solar cells: a critical review. *Energy Technol.*, 2021, **9**, 2100560.
[13] Zhao P., Han M., Yin W., Zhao X., Kim S.G., Yan Y., Kim M., Song Y. J., Park N.G., Jung H.S. Insulated interlayer for efficient and photostable electron-transport-layer-free perovskite solar cells. *ACS Appl. Mater. Interfaces*, 2018, **10**, P. 10132–10140.
[14] Kozlova E.A., Valeeva A.A., Sushnikova A.A., Zhurenok A.V., Rempel A.A. Photocatalytic activity of titanium dioxide produced by high-energy milling. *Nanosystems: Phys. Chem. Math.*, 2022, **13**, P. 632–639.
[15] Huang C., Lin P., Fu N., Liu C., Xu B., Sun K., Wang D., Zenga X., Ke S. Facile fabrication of highly efficient ETL-free perovskite solar cells with 20 % efficiency by defect passivation and interface engineering. *Chem. Commun.*, 2019, **55**, P. 2777–2788.
[16] Isikgor F.H., Zhumagal S., Merino L.V.T., De Bastiani M., McCulloch I., De Wolf S. Molecular engineering of contact interfaces for high-performance perovskite solar cells. *Nat. Rev. Mater.*, 2023, **8**, P. 89–108.
[17] Kozlov S.S., Alexeeva O.V., Nikolskaia A.B., Shevaleevskiy O.I., Averkiev D.D., Kozhuhovskaya P.V., Almjasheva O.V., Larina L.L. Double perovskite oxides La_2NiMnO_6 and $La_2Ni_{0.8}Fe_{0.2}MnO_6$ for inorganic perovskite solar cells. *Nanosystems: Phys. Chem. Math.*, 2022, **13**, P. 314–319.
[18] Nikolskaia A.B., Vildanova M.F., Kozlov S.S., Shevaleevskiy O.I. Physicochemical approaches for optimization of perovskite solar cell performance. *Russ. Chem. Bull.*, **69**, P. 1245–1252.
[19] Nikolskaia A.B., Kozlov S.S., Karyagina O.K., Alexeeva O.V., Almjasheva O.V., Averkiev D.D., Kozhuhovskaya P.V., Shevaleevskiy O.I. Cation doping of La_2NiMnO_6 complex oxide with the double perovskite structure for photovoltaic applications. *Russ. J. Inorg. Chem.*, 2022, **67**, P. 921–925.
[20] Han G., Zhang S., Boix P.P., Wong L.H., Sun L., Lien S.-Y. Towards high efficiency thin film solar cells. *Progr. Mater. Sci.*, 2017, **87**, P. 246–291.
[21] Sheikh M.S., Sakhya A.P., Dutta A., Sinha T.P. Light induced charge transport in La_2NiMnO_6 based Schottky diode. *J. Alloy. Comp.*, 2017, **727**, P. 238–245.
[22] Tauc J., Grigorovici R., Vancu A. Optical properties and electronic structure of amorphous germanium. *Phys. Status Solidi*, 1966, **15**, P. 627–637.

Submitted 15 September 2023; revised 10 October 2023; accepted 12 October 2023

Information about the authors:

Sergey S. Kozlov – Emanuel Institute of Biochemical Physics, Russian Academy of Sciences, Kosygin St., 4, Moscow, 119334, Russia; ORCID 0000-0002-8660-5646; sergeykozlov1@gmail.com

Anna B. Nikolskaia – Emanuel Institute of Biochemical Physics, Russian Academy of Sciences, Kosygin St., 4, Moscow, 119334, Russia; ORCID 0000-0002-7430-4133; anickolskaya@mail.ru

Olga K. Karyagina – Emanuel Institute of Biochemical Physics, Russian Academy of Sciences, Kosygin St., 4, Moscow, 119334, Russia; ORCID 0000-0002-6702-5195; olgakar07@mail.ru

Ekaterina K. Kosareva – N. N. Semenov Federal Research Center for Chemical Physics, Russian Academy of Science, Kosygin St., 4, Moscow, 119991, Russia; ORCID 0000-0001-8090-2052; catherine.kos@yandex.ru

Olga V. Alexeeva – Emanuel Institute of Biochemical Physics, Russian Academy of Sciences, Kosygin St., 4, Moscow, 119334, Russia; ORCID 0000-0001-8982-3959; alexol@yandex.ru

Vasilisa I. Petrova – Emanuel Institute of Biochemical Physics, Russian Academy of Sciences, Kosygin St., 4, Moscow, 119334, Russia; ORCID 0009-0001-6357-2052; balagur.sh@yandex.ru

Oksana V. Almjasheva – St. Petersburg State Electrotechnical University "LETI", Professora Popova St., 5, St. Petersburg, 197376, Russia; Ioffe Physical-Technical Institute, Russian Academy of Sciences, Politekhnicheskaya St., 26, St. Petersburg, 194021, Russia; ORCID 0000-0002-6132-4178; almjasheva@mail.ru

Oleg I. Shevaleevskiy – Emanuel Institute of Biochemical Physics, Russian Academy of Sciences, Kosygin St., 4, Moscow, 119334, Russia; ORCID 0000-0002-8593-3023; shevale2006@yahoo.com

Conflict of interest: the authors declare no conflict of interest.